Ultrathin Molybdenum Polyoxometalate−Polyelectrolyte Multilayer Films

Frank Caruso,*,† Dirk G. Kurth,† Dirk Volkmer,‡ Michael J. Koop,‡ and Achim Müller‡

Max-Planck-Institute of Colloids and Interfaces, Rudower Chaussee 5, D-12489 Berlin, Germany, and Fakultät für Chemie der Universität Bielefeld, Lehrstuhl für Anorganische Chemie I, Universitätsstrasse 25, D-33615 Bielefeld, Germany

Received February 12, 1998. In Final Form: April 8, 1998

Ultrathin multilayer films of a novel molybdenum(VI) polyoxometalate cluster ($(NH_4)_{21}[H_3Mo_{57}V_6(NO)_6O_{183}(H_2O)_{18}]$) ($Mo_{57}$) and poly(allylamine hydrochloride) (PAH) have been prepared by the consecutive stepwise adsorption of Mo_{57} and PAH from dilute aqueous solution. The Mo_{57}/PAH multilayer films have been characterized by optical spectroscopy and small-angle X-ray reflectivity (XR) methods. UV−vis measurements reveal regular film growth with each Mo_{57} adsorption. The average Mo_{57} surface density was found to be $(1.4 \pm 0.4) \times 10^{13}$ clusters per cm^2, corresponding to an average surface coverage of 56 ± 12%. XR experiments confirm uniform film growth, with the film thickness increasing with each Mo_{57} adsorption step. The average thickness for the Mo_{57}/PAH layer pair was determined to be 0.8 ± 0.1 nm. The Mo_{57} density in the film can be readily controlled by varying the polyelectrolyte interlayer separation between each Mo_{57} layer, and the total film thickness can be controlled by altering the number of adsorption cycles.

Introduction

The controlled incorporation of metal nanosized particles into a well-defined solid matrix is of widespread interest in materials science. Ordered assemblies of such composite materials have potential uses as electron-transfer materials for energy storage applications,[1,2] data storage systems,[3] optical gratings,[4] filters,[5] and coatings[6] and in the area of microelectronics.[3,7−9] Several techniques have been employed to produce solid-state assemblies of metal nanoparticles. Langmuir−Blodgett deposition has been used to construct ordered nanocomposite materials.[10] Ultrathin multilayer films of metal oxides have been prepared by means of a surface sol−gel process.[11] More recently, the preparation of ordered layers of gold nanoparticles within porous silica matrixes using a combination of colloidal adsorption and sol−gel processing techniques has been reported.[12] The layer-by-layer self-assembly method originally applied to produce multilayer assemblies of polymers[13−24] has also recently been used to produce various ordered metal−polymer composite films; multilayer films of colloidal gold, cadmium sulfide, lead sulfide, and titanium dioxide incorporated into polymer matrixes have been fabricated.[1,2,9,25,26] This technique, which involves the sequential adsorption of oppositely charged species from dilute solution, has been widely employed because of its simplicity and effectiveness in preparing multilayer films, as well as allowing the film composition and film thickness to be easily controlled.

Polyoxometalates are an attractive class of nanoparticles because of their particularly interesting nanosized structure[27,28] and their potential applications in the areas of catalysis, molecular electronics, and medicine.[29−31] Practical applications of polyoxometalates in these areas depend on the successful preparation of thin polyoxometalate-containing films. Ingersoll et al. employed cyclic

* To whom correspondence should be addressed. Fax: +49 30 6392 3102. E-mail: caruso@mpikg.fta-berlin.de.

† Max-Planck-Institute of Colloids and Interfaces.

‡ Fakultät für Chemie der Universität Bielefeld, Lehrstuhl für Anorganische Chemie.

(1) Schmitt, J.; Decher, G.; Dressick, W. J.; Brandow, S. L.; Geer, R. E.; Shashidhar, R.; Calvert, J. M. *Adv. Mater.* **1997**, *9*, 61.

(2) Feldheim, D. L.; Grabar, K. C.; Natan, M. J.; Mallouk, T. E. *J. Am. Chem. Soc.* **1996**, *118*, 7640.

(3) Hayashi, S.; Kumamoto, Y.; Suzuki, T.; Hirai, T. *J. Colloid Interface Sci.* **1991**, *144*, 538.

(4) Xia, Y.; Kim, E.; Mrksich, M.; Whitesides, G. M. *Chem. Mater.* **1996**, *8*, 601.

(5) Asher, S. A. US Patent 4,627,689; US Patent 4,632,517.

(6) Hinz, P.; Dislich, H. *J. Non-Cryst. Solids* **1986**, *82*, 411.

(7) Roescher, A.; Müller, M. *Adv. Mater.* **1995**, *7*, 151.

(8) Antonietti, M.; Wenz, E.; Bronstein, L.; Seregina, M. *Adv. Mater.* **1995**, *7*, 1000.

(9) Kotov, N. A.; Dekany, I.; Fendler, J. H. *J. Phys. Chem.* **1995**, *99*, 13065.

(10) Fendler, J. H.; Meldrum, F. C. *Adv. Mater.* **1995**, *7*, 607 and references therein.

(11) Ichinose, I.; Senzu, H.; Kunitake, T. *Chem. Lett.* **1996**, 831.

(12) Fan, H.; Zhou, Y.; Lopez, G. P. *Adv. Mater.* **1997**, *9*, 728.

(13) Decher, G.; Hong, J. D. *Makromol. Chem., Makromol. Symp.* **1991**, *46*, 321.

(14) Decher, G.; Hong, J. D. *Ber. Bunsen-Ges. Phys. Chem.* **1991**, *95*, 1430.

(15) Decher, G.; Hong, J. D.; Schmitt, J. *Thin Solid Films* **1992**, *210/211*, 831.

(16) Decher, G.; Schmitt, J. *Prog. Colloid Polym. Sci.* **1992**, *89*, 160.

(17) Lvov, Y.; Decher, G.; Möhwald, H. *Langmuir* **1993**, *9*, 481.

(18) Decher, G.; Lvov, Y.; Schmitt, J. *Thin Solid Films* **1994**, *244*, 772.

(19) Ferreira, M.; Rubner, M. F. *Macromolecules* **1995**, *28*, 7107.

(20) Fou, A. C.; Rubner, M. F. *Macromolecules* **1995**, *28*, 7115.

(21) Kellogg, G. J.; Mayes, A. M.; Stockton, W. B.; Ferreira, M.; Rubner, M. F.; Satija, S. K. *Langmuir* **1996**, *12*, 5109.

(22) Fou, A. C.; Onitsuka, O.; Ferreira, M.; Rubner, M. F.; Hsieh, B. R. *J. Appl. Phys.* **1996**, *79*, 7501.

(23) Cheung, J. H.; Stockton, W. B.; Rubner, M. F. *Macromolecules* **1997**, *30*, 2712.

(24) Caruso, F.; Niikura, K.; Furlong, D. N.; Okahata, Y. *Langmuir* **1997**, *13*, 3422.

(25) Gao, M.; Zhang, X.; Yang, B.; Li, F.; Shen, J. *Thin Solid Films* **1996**, *284*, 242.

(26) Musick, M. D.; Keating, C. D.; Keefe, M. H.; Natan, M. J. *Chem. Mater.* **1997**, *9*, 1499.

(27) Zhang, S.; Huang, G.; Shao, M.; Tang, Y. *J. Chem. Soc., Chem. Commun.* **1993**, 37.

(28) Müller, A.; Krickemeyer, E.; Dillinger, S.; Bögge, H.; Plass, W.; Proust, A.; Dloczik, L.; Menke, C.; Meyer, J.; Rohlfing, R. *Z. Anorg. Allg. Chem.* **1994**, *620*, 599.

(29) Pope, M. T.; Müller, A. *Angew. Chem.* **1991**, *103*, 56; *Angew. Chem., Int. Ed. Engl.* **1991**, *30*, 34. Pope, M. T. In *Heteropoly and Isopoly Oxometalates* (*Inorg. Chem. Concepts 8*); Springer: Berlin, 1983.

(30) Ingersoll, D.; Kulesza, P. J.; Faulkner, L. F. *J. Electrochem. Soc.* **1994,** *141*, 140.

(31) *Chem. Rev.* **1998**, *98*, 1. The entire issue is devoted to polyoxometalates.

S0743-7463(98)00177-2 CCC: $15.00
Published on Web 05/29/1998

voltammetry to demonstrate the formation of polyoxometalate-based layered films on conducting substrates; films of isopolymolybdate, phosphotungstate, or silicotungstate, alternating with various cationic species, were prepared.[30] That study focused mainly on the electrochemical properties of the films. More recently, Ichinose et al. fabricated multilayer films of molybdenum oxide and linear polycations.[32] Film formation was studied using a quartz crystal microbalance, and film structure was studied by scanning electron microscopy.[32] In that work, adsorption of the ammonium octamolybdate ($(NH_4)_4[Mo_8O_{26}]$) on poly(allylamine hydrochloride) (PAH) surfaces was found to proceed without saturation due to the consecutive precipitation of polyoxomolybdates as a result of condensation of the adsorbed octamolybdate species. The layer thickness depended on the adsorption time: the growth rate of the layer was 0.57 nm min^{-1}; film thicknesses were in the range 2−25 nm for the adsorption times employed, corresponding to 2−30 layers of the $[Mo_8O_{26}]^{4-}$ unit. In addition to the unique time-dependent characteristics observed for the adsorption of $(NH_4)_4[Mo_8O_{26}]$ on PAH, the formation of the multilayer films was found to critically depend on the pH of the polymer solutions. Multilayer films of the molybdenum oxide alternating with PAH could *not* be formed at pH values of about 5−6 for the PAH solution, but only at lower pH values (∼3). Further, molybdenum oxide/poly(ethyleneimine) (PEI) multilayer films could not be formed due to the high solubility of the molybdenum oxide/PEI complex, nor could multilayers of $[V_{10}O_{28}]^{6-}$/PAH.

In the present study, we report on the preparation of ultrathin multilayer polyoxometalate−polyelectrolyte films by the consecutive stepwise adsorption of a novel, well-characterized molybdenum polyoxometalate cluster ($(NH_4)_{21}[H_3Mo_{57}V_6(NO)_6O_{183}(H_2O)_{18}]$) ($Mo_{57}$) and poly(allylamine hydrochloride) (PAH). UV−vis spectroscopy and small-angle X-ray reflectivity (XR) are exploited for examining the growth, structure, and morphology of the composite Mo_{57}/PAH films. The external form of the Mo_{57} cluster resembles a flattened ellipsoid with dimensions 1.6 × 2.4 nm (determined from X-ray crystallography measurements). The electronic structure of these types of molybdenum polyoxometalate clusters has previously been investigated by MO calculations, by different spectroscopic methods, and magnetochemically,[33] and their structural diversity has only recently been recognized.[34] The wide-spread application of polyoxometalates based on the Keggin structure type in solid-state devices, catalysis, biochemistry, and medicine provides further impetus for investigation of this new class of molybdenum polyoxometalate clusters.[29]

Experimental Section

Materials. Poly(ethyleneimine) (PEI), MW 50 000, poly(sodium 4-styrenesulfonate) (PSS), MW 70 000, and poly(allylamine hydrochloride) (PAH), MW 8 000−11 000, were obtained from Aldrich. PEI and PAH were used as received, whereas PSS was dialyzed against Milli-Q water (MW cutoff 14 000) and lyophilized before use. The Mo_{57} cluster was synthesized by a modified synthetic route to that published:[28] A mixture of $(NH_4)_6[Mo_7O_{24}]\cdot 4H_2O$ (8.7 g, 7.0 mmol), $NH_2OH.HCl$ (4 g, 57.5 mmol), and NH_4Cl (4.32 g, 80.7 mmol) in 150 mL of H_2O was heated without stirring in a 300 mL wide-necked Erlenmeyer flask covered with a watch glass at 60 °C for 17 h. The hot solution was filtered and stored at room temperature. Red crystals of $(NH_4)_{12}[Mo_{36}(NO)_4O_{108}(H_2O)_{16}]\cdot 33H_2O$, which precipitated within 6 h, were filtered and air-dried. Yield: 7.9 g (91% rel. to Mo). Anal. Calcd for $H_{146}Mo_{36}N_{16}O_{161}$: H, 2.30; Mo, 53.96; N, 3.50. Found: H, 2.27; Mo, 53.3; N, 3.36. $(NH_4)_{12}[Mo_{36}(NO)_4O_{108}(H_2O)_{16}]\cdot 33H_2O$ (2 g, 0.312 mmol) was dissolved in 22 mL of a 0.5 M aqueous $VOCl_2$ solution at pH 1.0 and the resulting solution heated at 90 °C for 30 min. A brown precipitate was filtered from the hot solution, and NH_4Cl (0.5 g, 9.3 mmol) was dissolved in the purple filtrate. Purple hexagonal *crystals* of the Mo_{57} cluster deposited at room temperature within 3 days. Yield: 0.79 g (36% rel to Mo). Anal. Calcd for $H_{233}Mo_{57}N_{27}O_{262}V_6$: H, 2.21; Mo, 51.69; N, 3.57; V, 2.89. Found: H, 1.67; Mo, 51.52; N, 3.52; V, 2.76. Sodium chloride (AR grade) was purchased from Merck and used as received. Quartz slides (1.25 × 12 × 46 mm) were obtained from Hellma Optik GmbH. The water used in all experiments was prepared in a three-stage Millipore Milli-Q Plus 185 purification system and had a resistivity higher than 18.2 MΩ cm.

Film Preparation. Quartz slides were cleaned by immersion in a solution containing 1 part NH_4OH (29 wt % aqueous solution), 1 part H_2O_2 (30 wt % aqueous solution), and 5 parts pure water at 70 °C for 20 min, followed by rinsing with copious amounts of water (**warning**: *Mixtures of ammonium hydroxide and hydrogen peroxide are extremely corrosive and should be handled with great care*). The cleaned quartz substrates were then immersed in 10 mL of a 10^{-2} M PEI solution (based on the molecular weight of the monomer unit) for 20 min, rinsed by dipping them twice in pure water solutions for 2 min each, and dried with a gentle stream of argon. Multilayers were prepared by exposing the PEI-coated substrates to a 10^{-2} M PSS solution containing 1 M NaCl for 20 min, followed by alternating 20 min immersions in PAH (10^{-2} M containing 1 M NaCl, pH ∼ 5−6) and Mo_{57} (2×10^{-4} M, pH ∼ 3.5) solutions. (In some films where the polyelectrolyte interlayer separation was varied, the Mo_{57} deposition step was replaced by PSS deposition.) Water rinses and argon drying steps were performed after each adsorption step.

UV−vis and Small-Angle X-ray Reflectivity (XR) Measurements. UV−vis absorption spectra were recorded using a Cary Model 4E UV−visible spectrophotometer. XR experiments were performed with a commercial $\theta/2\theta$ instrument (STOE & CIE GmbH, Darmstadt, Germany) using copper Kα radiation (wavelength = 1.54 Å). The divergence of the incoming beam was 0.1°. Analysis of the XR data was performed with a box-model simulation as described elsewhere.[35] The error in the XR thickness and surface roughness data is ±0.2 nm. X-ray reflectivity measurements performed on multilayer films assembled on silicon wafers yielded data similar to those obtained for films on quartz substrates.

Results and Discussion

The formation of Mo_{57}/PAH multilayer films was first examined by UV−vis spectroscopy. Figure 1 displays the UV−vis absorption spectra of $(Mo_{57}/PAH)_n$ multilayers (with $n = 0-6$) assembled on a precursor PEI/PSS/PAH film on quartz substrates. The inset in Figure 1 shows the absorption spectrum of an aqueous Mo_{57} solution, as well as a polyhedral representation of the Mo_{57} cluster. The solution absorption spectrum of Mo_{57} exhibits a broad band in the 500−600 nm range, with a maximum at 558 nm. The extinction coefficient at 558 nm (ϵ_{558} ∼20 000 M^{-1} cm^{-1}) is 20 times smaller than ϵ_{225} (∼4×10^5 M^{-1} cm^{-1}). This explains the absence of a *strong* absorption band at 558 nm in the Mo_{57}/PAH multilayer film spectra. The absorption spectrum for the precursor multilayer film PEI/PSS/PAH ($n = 0$) shows a peak at 225 nm, which is due to the benzene chromophores in PSS. PAH does not absorb above 200 nm, and therefore its presence in the

(32) Ichinose, I.; Tagawa, H.; Mizuki, H.; Lvov, Y.; Kunitake, T. *Langmuir* **1998**, *14*, 187.

(33) Gatteschi, D.; Sessoli, R.; Plass, W.; Müller, A.; Krickemeyer, E.; Meyer, J.; Sölter, D.; Adler, P. *Inorg. Chem.* **1996**, *35*, 1926.

(34) Müller, A.; Plass, W.; Krickemeyer, E.; Dillinger, S.; Bögge, H.; Armatage, A.; Proust, A.; Beugholt, C.; Bergmann, U. *Angew. Chem.* **1994**, *106*, 897; *Angew. Chem., Int. Ed. Engl.* **1994**, *33*, 849. Müller, A.; Plass, W. *J. Mol. Struct.* **1994**, *321*, 215. Müller, A.; Bögge, H.; Krickemeyer, E.; Dillinger, S. *Bull. Pol. Ac. Sci. Chem.* **1994**, *42*, 292.

(35) Asmussen, A.; Riegler, H. *J. Chem. Phys.* **1996**, *104*, 8159.

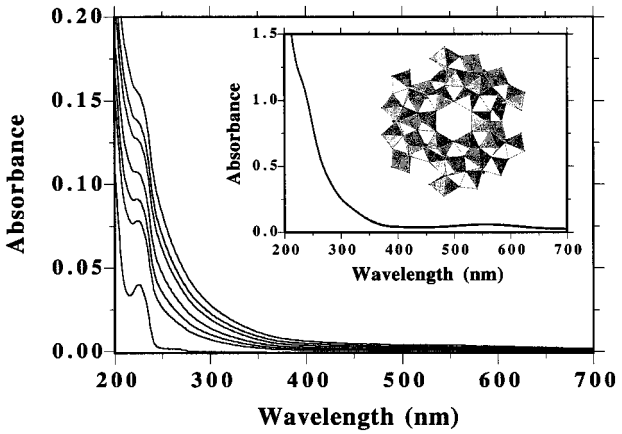

Figure 1. UV−vis absorption spectra of $(Mo_{57}/PAH)_n$ multilayer films with $n = 0-6$ on PEI/PSS/PAH-modified quartz substrates. The lowest curve corresponds to the precursor film ($n = 0$). The other curves, from bottom to top, correspond to $n = 1, 2, 3, 4, 5$, and 6, respectively. The inset shows the absorbance spectrum of an aqueous 0.033 mg mL^{-1} Mo_{57} solution (Mo_{57} concentration is 3×10^{-6} M) and a polyhedral representation of the Mo_{57} cluster.

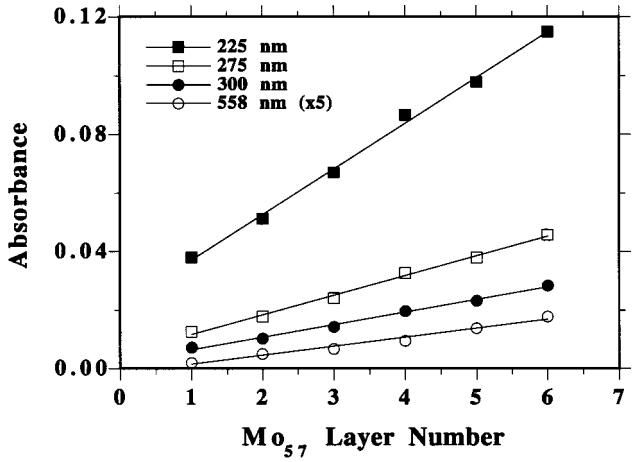

Figure 2. Plot of the absorbance values at 225, 275, 300, and 558 nm as a function of the number of Mo_{57} layers for the $(MO_{57}/PAH)_n$ multilayer films with $n = 0-6$ on PEI/PSS/PAH-modified quartz substrates. The absorbance at 558 nm has been multiplied by 5.

film is not reflected in the absorption spectra. The incorporation of Mo_{57} in the film is confirmed by the increase in absorbance in the 200−600 nm range with each additional deposition of Mo_{57} ($n = 1-6$). The spectra shown in Figure 1 are for multilayers that have an outer PAH layer, since some loss of Mo_{57} occurred at each step of PAH deposition (monitored via UV−vis measurements). Recent studies have also demonstrated a loss of polyoxometalate species,[32] or charged organic dye molecules,[36−38] upon subsequent exposure to a polyelectrolyte solution in the preparation of multilayer films.

The absorbance values for $(Mo_{57}/PAH)_n$ multilayer films with $n = 1-6$ at 225, 275, 300, and 558 nm are plotted as a function of the number of Mo_{57} layers in Figure 2. For films with $n > 1$, the absorbance varies linearly with layer number at all four wavelengths, which reveals a constant increase in the total amount of Mo_{57} remaining in the film after each exposure to PAH solution. Since ϵ at 558 nm for Mo_{57} is small, the absorbance data at 558 nm for the films have been multiplied by 5. The average absorbance values at 225, 275, 300, and 558 nm for $(Mo_{57}/PAH)_n$ multilayer films with $n > 1$ are 1.54×10^{-2}, 6.60×10^{-3}, 4.21×10^{-3}, and 5.93×10^{-4}, respectively. (These values are for films formed on *both* sides of the quartz substrates.) It can also be seen that the absorbance value corresponding to the deposition of Mo_{57} onto the precursor PEI/PSS/PAH film—and after exposure to PAH solution—is larger than those obtained for subsequent Mo_{57} depositions; extrapolation of linear regression curves toward $n = 0$ reveals that they do not pass through the origin. This reflects the greater amount of Mo_{57} immobilized by the precursor PEI/PSS/PAH film and may be explained by the nanosized particles penetrating the polyelectrolyte layers. For a precursor film of seven layers, PEI/$(PSS/PAH)_3$, an even larger absorbance of 0.053 at 225 nm for a single deposition of Mo_{57} is observed, compared with 0.037 at 225 nm for the three-layer film (PEI/PSS/PAH).

The surface density, Γ, of Mo_{57} on the PAH surface in the $(Mo_{57}/PAH)_n$ films can be calculated using $\Gamma = [(A_\lambda/2)\epsilon_\lambda^{-1}N_A] \times 10^{-3}$, where A_λ is the absorbance of Mo_{57} in the *film* at a given wavelength (λ), ϵ_λ is the extinction coefficient of Mo_{57} in solution (M^{-1} cm^{-1}) at λ, and N_A is Avogadro's number.[39] Using the absorbance values in the 200−300 nm range (where absorbance is largest) and the corresponding extinction coefficients calculated from the solution absorption spectrum of Mo_{57}, an average Mo_{57} surface density of $(1.4 \pm 0.4) \times 10^{13}$ clusters per cm^2 is obtained for $(Mo_{57}/PAH)_n$ multilayer films with $n > 1$. This corresponds to an average area per Mo_{57} of 7.1 ± 2.0 nm^2. Hence, assuming a single Mo_{57} cluster occupies an area of approximately 3.2−4.8 nm^2, depending on its relative orientation,[40] the average surface coverage is $56 \pm 12\%$. The average surface density for the first layer of Mo_{57} deposited onto the PEI/PAH/PSS precursor film is $(2.8 \pm 0.1) \times 10^{13}$ clusters per cm^2, which is twice that observed for subsequent layers of Mo_{57}. As discussed above, Mo_{57} penetrates the precursor layers, which explains the increased coverage observed. The surface coverage values for films with $n > 1$ are approximately a factor of 2 lower than those reported by Ingersoll et al. for *smaller* polyoxometalate particles on native and modified conducting surfaces[30] and more than 1 order of magnitude lower than those reported by Ichinose et al.[32] for ammonium octamolybdate ($(NH_4)_4[Mo_8O_{26}]$) on PAH, where much greater than monolayer amounts of the polyoxometalate species are deposited due to condensation of the adsorbed octamolybdate species.

The effect of polyelectrolyte interlayer separation (between each Mo_{57} layer) on the amount of Mo_{57} deposited was also examined. Increasing the polyelectrolyte interlayer separation between Mo_{57} layers from a single PAH layer to three layers (PAH/PSS/PAH) resulted in a larger amount of Mo_{57} being incorporated into the film. The average absorbance at 225 nm for these films from three experiments is 0.037 ± 0.04 (two sides), demonstrating that a constant amount of Mo_{57} is deposited with each step. Furthermore, the amount of Mo_{57} in precursor films of increasing thickness (one to seven layers) has no linear correlation to the number of polyelectrolyte layers−a

(36) Ariga, K.; Lvov, Y.; Kunitake, T. *J. Am. Chem. Soc.* **1997**, *119*, 2224.
(37) Ariga, K.; Onda, M.; Lvov, Y.; Kunitake, T. *Chem. Lett.* **1997**, 25.
(38) Linford, M.; Auch, M.; Möhwald, H. *J. Am. Chem. Soc.* **1998**, *120*, 178.
(39) Li, D.; Swanson, B. I.; Robinson, J. M.; Hoffbauer; M. A. *J. Am. Chem. Soc.* **1993**, *115*, 6975. The absorbance in the current work is divided by 2 to give a surface density for a single layer of Mo_{57}, since the quartz plate has film on both sides.
(40) The surface densities covering the (100), (010), and (001) crystallographic planes of the hexagonal crystal lattice of Mo_{57} are $\Gamma_{(100)} = \Gamma_{(010)} = 3.12 \times 10^{13}$ clusters cm^{-2}, and $\Gamma_{(001)} = 2.06 \times 10^{13}$ clusters cm^{-2}.

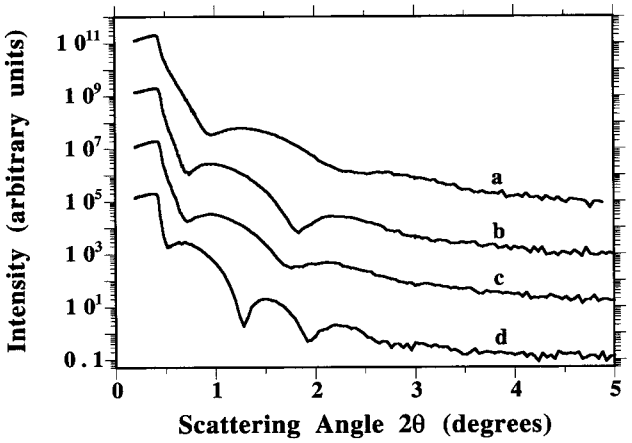

Figure 3. X-ray reflectivity curves of alternating Mo_{57}/PAH multilayer films on quartz substrates. The reflectivity curves have been recorded at different stages of film growth: (a) precursor film PEI/PSS/PAH; (b) PEI/PSS/PAH/Mo_{57}; (c) PEI/PSS/PAH/(Mo_{57}/PAH); (d) PEI/PSS/PAH/(Mo_{57}/PAH)$_6$. Individual curves are shifted in the *y*-axis direction for clarity.

plateau in the absorbance is approached around seven layers. This suggests that the polyelectrolyte multilayer films become more dense with increasing polyelectrolyte layer number, which is consistent with the notion that there is high overlap of individual layers in polyelectrolyte multilayers.[41]

XR experiments were performed in order to confirm the formation of Mo_{57}/PAH multilayer films and to investigate the film structure. The broad oscillations seen in each XR curve of the Mo_{57}/PAH multilayer films (Figure 3) are Kiessig fringes, which arise from X-ray interferences from the substrate−film and film−air interfaces. Bragg peaks, which are characteristic of ordered lattices, are observable in XR curves when the film has regions of sufficiently different electron density.[1] The absence of such peaks in the XR curves in Figure 3 indicates that the gradient of the refraction index between distinct layers is not large enough to resolve Bragg peaks. One explanation could be that the succession of Mo_{57} and polyelectrolyte regions in the multilayer films is not strictly lamellar with sharp interfacial confinements. The presence of Mo_{57} is confirmed by an increase in film electron density with an increasing number of Mo_{57} layers, as determined from analysis of the XR data. Evidence for multilayer film growth comes from the decrease in the distance between the Kiessig fringes (along the *x*-axis) in the XR curves as a result of Mo_{57} and PAH deposition. The thickness of the precursor film PEI/PSS/PAH on quartz (curve a) is 5.4 nm, with a surface roughness of 1.0 nm. The presence of Mo_{57} on the precursor film (curve b) increases the film thickness by 1.7 nm to a value of 7.1 nm and the surface roughness to 1.3 nm. Subsequent exposure of this film to a PAH solution produces a further increase in film thickness (7.5 nm) (curve c). From this value it is clear that an increase in the total film thickness occurs, even though PAH adsorption removes some preadsorbed Mo_{57} (assessed via UV−vis measurements). The surface roughness for the PEI/PSS/PAH/(Mo_{57}/PAH) film is 1.2 nm. The deposition of alternate Mo_{57} and PAH layers to give a PEI/PSS/PAH/(Mo_{57}/PAH)$_6$ film results in a film thickness of 11.6 nm, and a surface roughness of 1.3 nm (curve d). Thus, the average thickness for the Mo_{57}/PAH layer pair (for films with $n > 1$) is 0.8 ± 0.1 nm. Estimation of the thickness of a single Mo_{57} or PAH layer is complicated by the simultaneous removal of Mo_{57} and PAH deposition. Furthermore, the individual layer thicknesses for Mo_{57} and PAH layers cannot be reliably determined given the magnitude and error (±0.2 nm) in the experimental thicknesses. The reflectivity data, however, confirm the growth of Mo_{57}/PAH multilayer films. The average thickness obtained for the Mo_{57}/PAH layer pair is approximately 20 times smaller than that reported for the $[Mo_8O_{26}]^{4-}$ species (thickness ∼20 nm) for identical adsorption times of 20 min.[32] The thickness of 20 nm for $[Mo_8O_{26}]^{4-}$ corresponds to ca. 20 layers of the molybdate unit,[32] whereas in the current work less than a monolayer of Mo_{57} is deposited with each adsorption step. This also suggests that condensation of the Mo_{57} can be largely ruled out over the time frame of our experiments.

Atomic force microscopy (AFM) measurements of the (Mo_{57}/PAH)$_n$ films did not produce images in which individual Mo_{57} clusters could be clearly identified—largely due to the roughness of the polyelectrolyte film and the small size of the Mo_{57} clusters. However, the AFM surface roughness data for the multilayer films is in excellent *quantitative* agreement with that obtained from X-ray reflectivity measurements. The surface roughness of the Mo_{57}/PAH films (ca. 1 nm) is considerably less than the roughness of ∼10 nm reported for $[Mo_8O_{26}]^{4-}$/PAH multilayer films.[32]

Conclusions

The present work demonstrates the successful consecutive stepwise assembly of a new class of nanosized molybdenum polyoxometalate clusters, and PAH, to produce composite multilayer films: nanocomposite supramolecular films of controlled thickness and Mo_{57} density have been prepared. The control of such parameters is crucial in the development of nanostructured functional materials where molecular components are required to be integrated in an ordered macroscopic film.

Acknowledgment. Frank Caruso and Dirk Volkmer thank the Alexander von Humboldt Foundation and the Fonds der Chemischen Industrie, respectively, for research fellowships. Achim Müller thanks the Deutsche Forschungsgemeinschaft for financial support. The authors are grateful to Dr. Mohammed Ibn Elhaj for help with analysis of the X-ray reflectivity data and to Professor Helmuth Möhwald for valuable discussions.

Supporting Information Available: Packing plots of $[H_3Mo_{57}V_6(NO)_6O_{183}(H_2O)_{18}]^{21-}$ clusters within the (100) and (001) crystallographic planes (3 pages). Ordering information is given on any current masthead page.

LA980177V

(41) Decher, G. *Science* **1997**, *277*, 1232.